JOURNAL OF GEOPHYSICAL RESEARCH, VOL. 107, NO. D23, 4707, doi:10.1029/2002JD002415, 2002

Potential for photochemical ozone formation in the troposphere over the North Atlantic as derived from aircraft observations during ACSOE

Claire E. Reeves,[1] Stuart A. Penkett,[1] Stephane Bauguitte,[1,2] Kathy S. Law,[3]
Mathew J. Evans,[3,4] Brian J. Bandy,[1] Paul S. Monks,[5] Gavin D. Edwards,[5,6]
Gavin Phillips,[5] Hannah Barjat,[7,8] Joss Kent,[7] Ken Dewey,[7] Sandra Schmitgen,[9,10]
and Dieter Kley[9]

Received 4 April 2002; revised 9 August 2002; accepted 13 August 2002; published 11 December 2002.

[1] In this paper, ozone (O_3), water vapor (H_2O), carbon monoxide (CO), and peroxide concentrations and photolysis rates measured in the troposphere over the North Atlantic during two Atmospheric Chemistry Studies in the Oceanic Environment (ACSOE) aircraft field campaigns are used to calculate the concentration of nitric oxide (NO) required for net photochemical O_3 production (nP_{O3}) to be positive (NO_{comp}). NO_{comp} tended to show a decrease with altitude, although it was sometimes found to be low in the marine boundary layer (MBL) where H_2O concentrations were high and O_3 concentrations were low. nP_{O3} was calculated for the spring when NO data were available and was found to be mostly negative and generally increased from about -0.5 to -0.2 ppbv hr^{-1} in the MBL to $+0.04$ ppbv hr^{-1} at about 7–8 km altitude. The results suggest that much of the lower and middle troposphere over the eastern North Atlantic during spring is in a state of slow net photochemical O_3 destruction. However, in the upper troposphere, the system changes to one of net photochemical production, which results from the drier environment and higher NO concentrations. Furthermore, examples of net O_3 production were also observed in the lower and middle troposphere associated with either in situ sources of NO or long-range transport of pollution. The paper also illustrates the sensitivity of this O_3 production/loss state to H_2O and NO concentrations, photolysis rates, and temperatures. *INDEX TERMS:* 0365 Atmospheric Composition and Structure: Troposphere—composition and chemistry; 0368 Atmospheric Composition and Structure: Troposphere—constituent transport and chemistry; 9325 Information Related to Geographic Region: Atlantic Ocean; *KEYWORDS:* photochemical ozone formation, North Atlantic, aircraft observations

Citation: Reeves, C. E., et al., Potential for photochemical ozone formation in the troposphere over the North Atlantic as derived from aircraft observations during ACSOE, *J. Geophys. Res.*, *107*(D23), 4707, doi:10.1029/2002JD002415, 2002.

1. Introduction

[2] In the troposphere, one of the major loss processes for ozone (O_3) is its photolysis in the presence of water vapor (H_2O) leading to the formation of 2 hydroxyl radicals (OH).

$$O_3 + h\nu \rightarrow O(^1D) + O_2 \tag{1}$$

$$O(^1D) + H_2O \rightarrow 2OH \tag{2}$$

[3] Not only is this an important sink for O_3 but it is also the primary source of tropospheric OH [*Levy*, 1971]. The OH radicals can react with many species, including O_3 thereby acting as a further sink for O_3.

$$OH + O_3 \rightarrow HO_2 + O_2 \tag{3}$$

---

[1] School of Environmental Sciences, University of East Anglia, Norwich, UK.
[2] Now at British Antarctic Survey, Cambridge, UK.
[3] Centre for Atmospheric Science, University of Cambridge, Cambridge, UK.
[4] Now at Department of Engineering and Applied Science, Harvard University, Cambridge, MA, USA.
[5] School of Chemistry, University of Leicester, Leicester, UK.
[6] Now at Atmospheric Chemistry Division, National Center for Atmospheric Research, Boulder, CO, USA.
[7] Meteorological Research Flight, UK Meteorological Office, Farnborough, UK.
[8] Atmospheric Research Airborne Support Facility, Natural Environment Research Council, Swindon, UK.
[9] Institut für Chemie und Dynamik der Geosphære, Forschungszentrum Jülich, Jülich, Germany.
[10] Now at Laboratoire des Sciences du Climat et de L'Environment, UMR CEA/CNRS, Gif-sur-Yvette, France.

0148-0227/02/2002JD002415

[4] However OH reacts primarily with carbon monoxide (CO) and hydrocarbons to produce peroxy radicals (HO_2 and RO_2), which can react with nitric oxide (NO) and, in the case of HO_2, react with O_3.

$$OH + CO \rightarrow HO_2 + CO_2 \tag{4}$$

$$OH + CH_4 + O_2 \rightarrow CH_3O_2 + H_2O \tag{5}$$

$$HO_2 + NO \rightarrow NO_2 + OH \tag{6}$$

$$CH_3O_2 + NO + O_2 \rightarrow NO_2 + HCHO + HO_2 \tag{7}$$

$$HO_2 + O_3 \rightarrow OH + 2O_2 \tag{8}$$

[5] Reaction (8) is another sink for O_3, while reactions (6) and (7) produce nitrogen dioxide (NO_2), which *via* photolysis gives $O(^3P)$, thereby forming O_3 following reaction with O_2.

$$NO_2 + h\nu \rightarrow NO + O\left(^3P\right) \tag{9}$$

$$O\left(^3P\right) + O_2 \rightarrow O_3 \tag{10}$$

[6] Above a certain NO concentration (known as the NO compensation point (NO_{comp})), a cycle of reactions involving free radicals and NO_X ($NO + NO_2$) can occur in which the amount of O_3 produced (P_{O3}) (i.e., the reaction of the peroxy radicals with NO to form NO_2 (e.g., reactions (6) and (7)) exceeds the total amount destroyed via photolysis and reaction with OH and HO_2 (L_{O3}), giving net photochemical production of O_3.

[7] There are a number of processes involved in the photochemistry of O_3 upon which NO_{comp} is dependent. The rate of O_3 loss (ppbv hr^{-1}) is a function of the O_3 concentration. Clearly, the photolytic loss of O_3 is highly dependent on the H_2O concentration. Furthermore, since the reaction of $O(^1D)$ with H_2O is the major source of OH and subsequently HO_2 and RO_2, then all 3 loss processes and the production process are also in some way dependent on H_2O concentration.

[8] *Carpenter et al.* [1997] and *Cox* [1999] discussed how NO_{comp} varied between two marine boundary layer (MBL) sites, one in the Northern Hemisphere (Mace Head, Ireland) and the other in the Southern Hemisphere (Cape Grim, Tasmania) as a result of the different background concentrations of O_3. H_2O concentrations vary greatly between the MBL and the free troposphere, as well as between different layers (air masses) within the free troposphere [*Penkett et al.*, 1995, 1998]. Using data collected over the Pacific during the PEM-West A experiment, *Davis et al.* [1996] found that net photochemical O_3 production (nP_{O3}) increased with increasing altitude because of large decreases in L_{O3} with only moderate decreases in P_{O3}. The H_2O concentration was found to be the major controlling chemical factor in the decrease in L_{O3} with altitude. Typically, at altitudes below 6 km, high concentrations of H_2O and low concentrations of NO led to negative values of nP_{O3}. Conversely for altitudes above 6 km low concentrations of H_2O and high concentrations of NO led to positive values of nP_{O3}. *Davis et al.* [1996] also calculated NO_{comp} for 12 altitude data bins and found no simple trend except perhaps for the western North Pacific rim (WNPR) above 1 km where there was a trend of decreasing NO_{comp} with increasing altitude.

[9] *Klonecki and Levy* [1997] examined the effect of NO_X, O_3, temperature, and humidity on nP_{O3} and NO_{comp} and subsequently the expected variations with altitude, latitude, and season using a photochemical box model. Lower temperature and specific humidity caused NO_{comp} to be lower and these factors were consequently largely responsible for lower values of nP_{O3} at higher latitudes and in winter. *Klonecki and Levy* [1997] also used their box model to calculate nP_{O3} and NO_{comp} for a simulation performed with a three-dimensional global chemistry transport model (GCTM). In the lower and middle troposphere over remote oceanic regions, nP_{O3} was calculated to be negative, while in the upper troposphere net photochemical O_3 production values were generally small but positive and NO_{comp} lower. *Yienger et al.* [1999] continued this work to evaluate the role of chemistry in the winter–spring O_3 maximum observed in the northern midlatitude free troposphere. Below 500 mb, using the GCTM, the atmosphere was calculated to switch from a regime of net photochemical O_3 loss in the summer to nP_{O3} in the winter and spring. In winter NO_{comp} was lower, while the NO_X concentrations in remote regions were larger as a result of NO_X having a longer lifetime allowing greater transport from source regions. nP_{O3} maximized in early spring due to increased insolation, while the atmosphere was still relatively dry and NO_X concentrations high.

[10] In this paper measurements of O_3, H_2O, CO, and peroxide concentrations and photolysis rates made in the troposphere over the North Atlantic during two aircraft field campaigns in the spring and summer of 1997 as part of the Atmospheric Chemistry Studies in the Oceanic Environment (ACSOE) program have been used to calculate the concentration of NO required for net O_3 production to occur. This compensation point is mostly examined in terms of NO, because it is its reaction with the peroxy radicals that determines the rate of production of O_3 at any given time. However, because the concentration of NO, or more specifically the NO/NO_2 ratio, varies with time of day and altitude, largely due to the varying photolysis of NO_2, this compensation point is also discussed in terms of NO_X (NO_{Xcomp}). Where NO observations were available nP_{O3} (i.e., $P_{O3} - L_{O3}$) was also calculated. The results have been examined in terms of air mass type and history as identified by chemical tracers and back trajectory calculations.

[11] The paper is organized such that the field measurements are briefly described, followed by a description of the model used. The results are discussed firstly in terms of average vertical profiles of NO_{comp} and nP_{O3} and then some case studies are presented. The sensitivity of the results to uncertainties in $j(O(^1D))$ and NO are discussed before the conclusions.

2. Experiment

[12] As part of the ACSOE program two aircraft field campaigns took place over the North Atlantic based out of the Azores (Santa Maria, 37°N, 25°W) during April and September 1997. The campaigns involved 8 science flights of the UK Meteorological Research Flight C-130 aircraft, 3 in April and 5 in September, the tracks of which are shown in Figure 1.

[13] Temperature was measured by a Rosemount platinum resistance thermometer to an accuracy of 0.1°C with dew point measured to an accuracy of 0.25°–1°C depending on altitude using a General Eastern thermoelectric

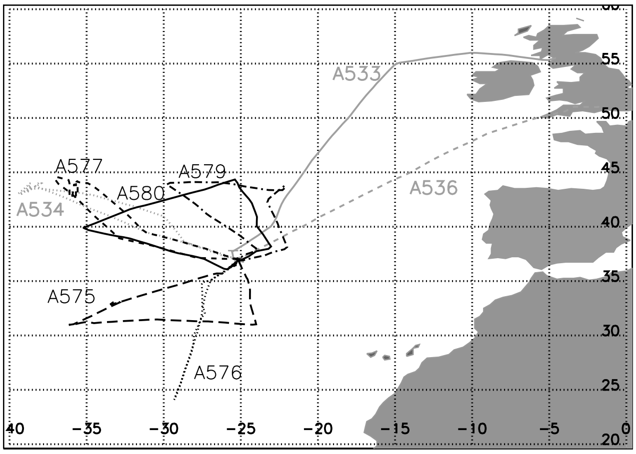

Figure 1. Flight tracks of the C-130 aircraft during the 2 ACSOE campaigns based in the Azores during April (gray) and September 1997 (black): A533 solid; A534 dots; A536 dashes; A575 long dashes; A576 dots; A577 dashes; A579 dash dots; A580 solid.

hygrometer. H_2O concentrations were calculated from the temperature, dew point and static pressure measured by capacitance to ±0.3% accuracy. O_3 was measured by ultraviolet absorption with a detection limit of 1 ppbv for an integration time of 1 s. CO was measured by fluorescence with an accuracy of 3% at a 1 s time resolution as described by *Gerbig et al.* [1999] in the summer while in the spring grab samples were collected in tedlar bags, which were subsequently analyzed (in duplicate) using an ANATROL RGA-3 analyzer (Cape, personal communication, 2001). The photolysis frequency for NO_2 was measured on the aircraft using two 2πsr fixed-bandwidth filter radiometers as described by *Volz-Thomas et al.* [1996] with a total error of 6%.

[14] NO was measured using a four-channel chemiluminescence analyzer designed and constructed in a collaborative project with the NOAA Aeronomy Laboratory in 1995/1996, since then operated at the University of East Anglia. The airborne instrument is described in detail by *Bauguitte* [2000]. The 1σ detection limit of the 1 s frequency data was estimated at 6 pptv (or 1 pptv for 1 min averages) from the photon counting statistics of the background/zero count rate of the detector (see Experimental in the work of *Carpenter et al.* [2000]). Background/zero levels were corrected for H_2O vapor changes for flights A533 and A534, but not A536 where the H_2O concentration did not vary over a large range. The average artifacts (or fake NO observed in zero air) derived for each flight are 4.7 (A533), 8.1 (A534), and 5.7 (A536) pptv. The effects of the uncertainties in these artifacts on the model results are examined in section 5.2. The overall uncertainty of the NO data, estimated from the propagation of systematic errors (mass flow controllers and NO/N_2 NIST traceable gas standard) and an error of 50% on the artifact level determination is ±21% for a 25 pptv NO ambient level. The NO data presented in this paper was smoothed using a 1 min running (box) average of the 1 s frequency primary data (maintaining the 1 s frequency). Subsequently, data points below detection limit were replaced by 1/2 the detection limit (0.5 pptv) to retain data coverage.

[15] Peroxide was removed from the air within a stripping coil, involved in an enzyme catalyzed reaction, the dimeric product of which was subsequently measured by fluorimetry [*Penkett et al.*, 1998]. Differentiation between inorganic (H_2O_2) and organic peroxide was made possible by the difference in the solubility of hydrogen and organic peroxides and by use of two stripping coils in series. The organic peroxide is assumed to be methyl hydrogen peroxide (CH_3OOH) for the purposes of constraining the photochemical model (see section 3).

3. Model

[16] The model is designed to calculate instantaneous O_3 production and loss rates constrained by measured in situ photolysis rates and observed concentrations of O_3, H_2O, CO, H_2O_2, and CH_3OOH. Five chemical continuity equations, 1 for each of the 5 chemical species to be calculated in the model (OH, HO_2, CH_3O_2, CH_3OH, NO_2), were set up assuming steady state (Concentration = Production/Loss) and the reactions listed in Table 1. For every 2 s period along the flight track where measured values for O_3, H_2O, CO, peroxides, j(NO_2), pressure, and temperature were available, the model was used to calculate the solutions to these equations. Since the concentrations of these species are dependent on one another, the solutions of the equations are interdependent and were thus solved iteratively based on an initial guess. The model reached a final solution when the results differed from those of the previous step by less than 0.1%. The final solution was insensitive to the initial guess.

[17] Since no in situ measurements of CO were available for the April flights, its concentration was set to a value of 133 ppbv, along the whole of the spring flight tracks, based on the analysis of the infrequent grab samples. Similarly, the data coverage of observed formaldehyde (HCHO) concentrations was low so its concentration was set at a 300 pptv, based on those measurements that were made (Mills, personal communication, 2001) and on other reported HCHO measurements made at a similar time in the North Atlantic [*Frost et al.*, 2002]. CH_4 concentrations were set at 1800 ppbv.

[18] Rates of photolytic reactions were calculated using the Madronich Tropospheric Ultraviolet-Visible radiation model (TUV Version 4.1.) (http://acd.ucar.edu/models/UV/TUV/index.html model) [*Madronich and Flocke*, 1998] at minute intervals along each flight track, thus considering altitude, latitude, longitude and time of day. The O_3 column was set at the value observed by TOMS (Total Ozone Mapping Spectrometer) at the median latitude and longitude of each flight. Cloud free conditions were assumed. The photolysis of NO_2 to NO (j(NO_2)) was constrained in the chemical model by measured in situ rates, while the rates of the other photolytic reactions were scaled to the observed rates of j(NO_2), based on their TUV model calculated ratio with j(NO_2), interpolated to the time of the observed j(NO_2). The average scale factors (j(NO_2)/j(X)) were 365, 1353, 1160, and 265 where X is O_3 ($\rightarrow O(^1D)$), H_2O_2, CH_3OOH and HCHO (→H + CHO). Thus the photolysis rates all varied with location, time of day and cloud cover. The exception to this was flight A575 on 14 September 1997 when no observed values of j(NO_2) were available and all photolysis rates were calculated along the flight track from

Table 1. Model Reactions and Rates

No.	Equation	Rate expression[a]
1	$O_3 + h\nu \rightarrow O(^1D) + O_2$	
2	$O(^1D) + M \rightarrow O(^3P)$	2.1×10^{-11} * exp(100/T)
3	$O(^1D) + H_2O \rightarrow 2OH$	2.2×10^{-10}
4	$OH + O_3 \rightarrow HO_2 + O_2$	1.5×10^{-12} * exp(−880/T)
5	$OH + CO \rightarrow HO_2 + CO_2$	1.5×10^{-13} * (1 + 0.6 * (P/1000))
6	$OH + CH_4 \rightarrow CH_3O_2 + H_2O$	2.45×10^{-12} * exp(−1775/T)
7	$HO_2 + NO \rightarrow NO_2 + OH$	3.5×10^{-12} * exp(250/T)
8	$CH_3O_2 + NO \rightarrow NO_2 + HCHO + HO_2$	3.0×10^{-12} * exp(280/T)
9	$HO_2 + O_3 \rightarrow OH + 2O_2$	2.0×10^{-14} * exp(−680/T)
10	$NO_2 + h\nu \rightarrow NO + O(^3P)$	
11	$HO_2 + HO_2 \rightarrow H_2O_2 + O_2$	(2.3×10^{-13} * exp(600/T) + 1.7×10^{-33} * M * exp(1000/T)) * (1+1.4×10^{-21} * H2O * exp(2200/T))
12	$CH_3O_2 + CH_3O_2 \rightarrow 0.6HO_2 + 1.3HCHO + 0.7CH_3OH$	2.5×10^{-13} * exp(190/T)
13	$HO_2 + CH_3O_2 \rightarrow CH_3OOH + O_2$	3.8×10^{-13} * exp(800/T)
14	$H_2O_2 + h\nu \rightarrow 2OH$	
15	$H_2O_2 + OH \rightarrow HO_2 + H_2O$	2.9×10^{-12} * exp(−160/T)
16	$CH_3OOH + h\nu \rightarrow HCHO + HO_2 + OH$	
17	$CH_3OOH + OH \rightarrow 0.7CH_3O_2 + 0.3HCHO + 0.3OH$	3.8×10^{-12} * exp(200/T)
18	$OH + HO2 \rightarrow H_2O + O_2$	4.8×10^{-11} * exp(250/T)
19	$HCHO + OH \rightarrow HO_2 + CO$	1.0×10^{-11}
20	$HCHO + h\nu \rightarrow 2HO_2 + CO$	
21	$OH + NO_2 \rightarrow HNO_3$	k0 = 2.4×10^{-30} * $(T/300)^{-3.1}$ kinf = 1.7×10^{-11} * $(T/300)^{-2.1}$[b]
22	$NO + O_3 \rightarrow NO_2 + O_2$	3.0×10^{-12} * exp(−1500/T)
23	$CH_3OH + OH + O_2 \rightarrow HCHO + HO_2 + H_2O$	6.7×10^{-12} * exp(−600/T)

[a] Rate expressions (k) are given in $cm^3\ mol^{-1}\ s^{-1}$ and are taken from the works of *DeMore et al.* [1997] and *Sander et al.* [2000]. T is absolute temperature (K). M is concentration of air molecules (mol cm^{-3}). P is pressure in mbars. Photolysis rates are assigned as described in the text.

[b] Calculated using Troe expression.

the TUV model, assuming clear sky conditions. The uncertainties of the results to the $j(NO_2)/j(O(^1D))$ ratio are examined by some sensitivity runs presented in section 5.1.

[19] NO was assigned in the model in different ways depending on the aim of the model runs. When calculations of the in situ values of P_{O3}, L_{O3}, and nP_{O3} were made, in situ measurements of NO were used to constrain the model. To calculate NO_{comp}, for each data point NO was initialized at 1 pptv, then incremented by 1 pptv until the value at which nP_{O3} was closest to zero was found. NO_{Xcomp} was simply the sum of NO_{comp} and the NO_2 mixing ratio calculated for that concentration of NO.

[20] The model does not take into account multiphase chemistry or rain out. The aircraft flight tracks were deliberately designed and executed to be in cloud free conditions, both along and above and below the flight path, where possible. However, it is possible that the air sampled may have been influenced by cloud in the previous few days. The flights were also over a remote oceanic region where the concentrations of nonmethane hydrocarbons and aerosols would be expected to be low. However, these omissions from the model must be borne in mind. Also it should be noted that the O_3 production and loss terms calculated here are for photochemical processes only.

4. Results and Discussion

[21] To examine the general features, the results are initially presented as average vertical profiles, produced by grouping the data into 500 m altitude bins. In doing so data from different times of day and latitude are all grouped together and some altitude bins may be strongly influenced by a single air mass sampled at a particular time or place. This is especially true for the spring data, where there were only 3 flights and few vertical profiles flown. Subsequently case studies are used to examine some of the processes that affect these average profiles.

4.1. NO Compensation Point

[22] On average NO_{comp} showed no clear correlation with altitude in the lowest 4 km of the atmosphere with values mostly between 15 and 25 pptv, but above this height they decreased with increasing altitude toward the top of the profiles (10–15 pptv at 6–8 km) (Figure 2). This would appear to be somewhat similar to the results over the Pacific where for PEM-West A no simple trend was found, except in the case of the WNPR region where for altitudes above 1 km there was a trend of decreasing NO_{comp} with increasing

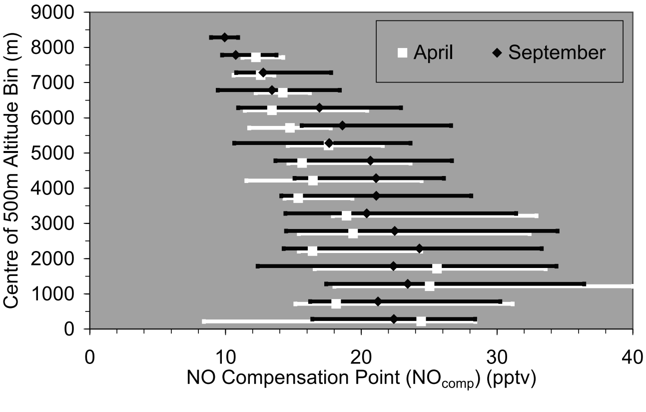

Figure 2. Mean NO_{comp} values calculated for 500 m altitude bins for the April (white squares) and September (black diamonds) flights. The bars indicate the 10th and 90th percentiles.

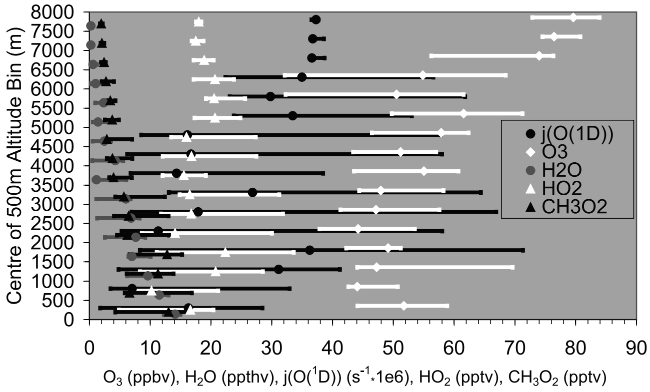

Figure 3. Median values for 500 m altitude bins for the April flights: observed O_3 (white diamonds), observed H_2O (gray dots), calculated $j(O(^1D))$ (black dots), calculated HO_2 (white triangles), calculated CH_3O_2 (black triangles). The bars indicate the 10th and 90th percentiles.

altitude [*Davis et al.*, 1996]. This relationship of decreasing NO_{comp} with increasing altitude is in agreement with that calculated by *Klonecki and Levy* [1997].

[23] The reason for this observed pattern of NO_{comp} with altitude is a function of a number of competing factors, which will be illustrated by examining the fluxes through individual O_3 loss reactions as calculated for the spring flights. First, it should be noted that the flux through any reaction between two molecules with constant mixing ratios decreases with altitude, simply due to the lower air density and thus lower number density of the reactants. However, NO_{comp}, given as a mixing ratio, should be the same at any altitude given the same reaction rates and mixing ratios for those species involved in O_3 loss.

[24] Second, the amount of O_3 lost via any reaction is directly and positively correlated to the O_3 concentration. The mixing ratio of O_3 during the spring flights, on average, did not vary much with height below 6.5 km, remaining mostly between 40 and 60 ppbv. Above this height, the average O_3 mixing ratio increased to between 70 and 80 ppbv (Figure 3), the direct effect of which is to tend toward a higher value of NO_{comp}, above 6 km, but only by, at most, a factor of 2.

[25] The flux through the photolysis of O_3, followed by reaction of $O(^1D)$ with H_2O, is not only a function of the O_3 concentration, but also the H_2O concentration and photolysis rate $j(O(^1D))$. The $j(O(^1D))$ values, derived from the measured $j(NO_2)$ values (see section 3), showed a lot of variability below 5 km. Above this height the mean values were consistently high, although not much higher than the highest mean values at the lower altitudes (Figure 3). H_2O mixing ratios, on the other hand, show a decline with altitude, by more than a factor of 10 between the lowest 500 m bin and above 6 km (Figure 3). The differences in H_2O concentrations therefore dominate, such that the changes in this reaction pathway tend toward lower values of NO_{comp} at higher altitudes. The loss of O_3 through this pathway is calculated to account for 50 to 60% of the total loss below about 3 km (Figure 4).

[26] Reaction with HO_2 is the next largest O_3 loss term, accounting for around 25–40% of the total loss below about 3 km, rising to 50–65% above 6 km where it is the dominant loss reaction (Figure 4). HO_2 is calculated to make up 55–90% (increasing with altitude) of the sum of HO_2 plus CH_3O_2 (Figure 3). Therefore, since the production of O_3 is via the reaction of NO with the peroxy radicals, the effect of changes in HO_2 concentration on L_{O3} is largely counterbalanced by its effect on P_{O3} and thus has very little effect on NO_{comp}. However, the effect of the decrease in temperature between the surface and about 8 km altitude will lead to an decrease in the flux through the reaction of HO_2 with O_3 by almost a factor of two, along with a slight increase in the rate of reaction between NO and the peroxy radicals. Changes to both these reaction rates lead to a decrease in NO_{comp} of about a factor of two.

[27] Therefore the large decrease in H_2O concentrations and the decrease in temperature lead to lower values of NO_{comp} at higher altitudes, which is only partially counterbalanced by the increase in O_3 concentrations. However, despite this general trend, there is no clear relationship below 4 km altitude in the calculated values of NO_{comp}, and considerable variability particularly at the lower altitudes.

[28] This variability is illustrated by the many individual vertical profiles that together make up the average profiles. On occasions NO_{comp} decreases with increasing altitude (e.g., profile 3 of flight A534 on 7 April 1997) (Figure 5a), while at other times it increases with increasing altitude (e.g., profile 4 of flight A576 on 16 September 1997) (Figure 5b). Often NO_{comp} displayed a maximum at about 1–3 km altitude, with minimums in the MBL and at the top of the profiles (6–8 km) (e.g., profile 3 of flight A533 on 7 April 1997) (Figure 5c). It is quite possible that above the maximum altitude flown by the aircraft in these latter 2 profiles, NO_{comp} would have continued to decrease with altitude, but clearly the pattern in the lower and middle troposphere is not simply one of decreasing NO_{comp} with increasing altitude.

[29] This is partly because O_3 and H_2O concentrations often do not exhibit monotonic variations with altitude. Furthermore, there can be much variability in the O_3

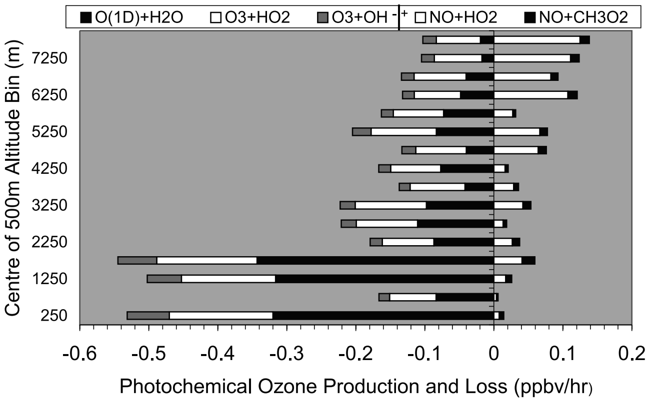

Figure 4. O_3 production and loss pathways, median values for 500 m altitude bins for the April flights: reaction of O_3 with OH (negative gray bar), reaction of O_3 with HO_2 (negative white bar), reaction of $O(^1D)$ with H_2O (negative black bar), reaction of NO with HO_2 (positive white bar), reaction of NO with CH_3O_2 (positive black bar).

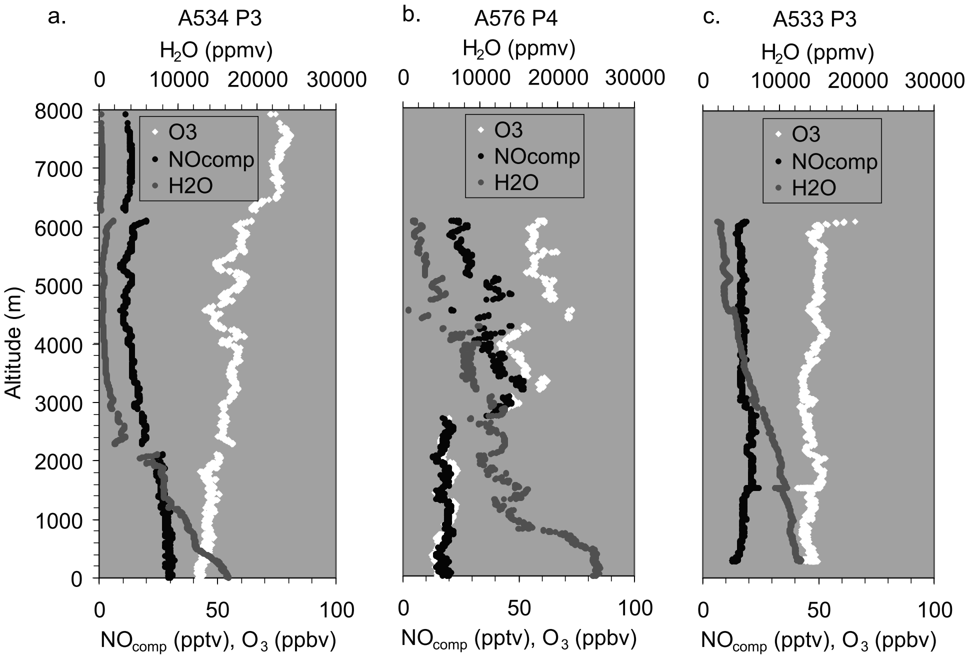

Figure 5. Vertical profiles of observed H_2O (gray dots) and O_3 (white diamonds) concentrations and calculated values of NO_{comp} (black dots): (a) profile 3 of flight A534 on 7 April 1997, (b) profile 4 of flight A576 on 16 September 1997, and (c) profile 2 of flight A576 on 16 September 1997.

concentration observed for any given H_2O concentration. This is likely to be related to the different origins and histories of the sampled air masses. MBL air can be lifted up into the free troposphere, while upper tropospheric air can be brought down into the middle or lower troposphere, with each air mass initially retaining some of its original identity. This can result in a very stratified troposphere, often with moist, O_3 poor layers overlaying dry, O_3 rich layers [*Newell et al.*, 1996; *Penkett et al.*, 1995, 1998]. Furthermore, H_2O concentrations may be altered by condensation or evaporation, while O_3 concentrations are unchanged, and, conversely, photochemistry may change O_3 concentrations, while the H_2O concentrations are unaltered. Some case studies are presented below in section 4.3 where some of these ideas will be examined in more detail.

[30] Figure 2 also illustrates that the calculated mean values of NO_{comp} are generally higher for the September flights than for the April fights. This agrees with the results of *Yienger et al.* [1999] who calculated that the O_3 loss is greater in September that April, due to more H_2O being present in September. The H_2O concentrations measured in the September flights were on average higher than those in April throughout the whole of the vertical column sampled [*Edwards*, 2000].

[31] Figure 6 shows how NO_{Xcomp} and the NO/NO_2 ratio vary with altitude. Unlike NO_{comp}, which shows no clear vertical gradient below 4 km altitude, NO_{Xcomp}, decreases with altitude throughout the whole profile. The NO_2 concentrations in these model runs are largely dependent on its rate of formation through the reaction of NO with O_3 and its rate of loss via photodissociation. Since the reaction between NO and O_3 decreases with temperature and the value of $j(NO_2)$ generally increases with altitude, the amount of NO_2 that can be sustained by the prescribed concentration of NO decreases with altitude, i.e., the internal balance of NO_X shifts toward the NO and the NO/NO_2 ratio increases with altitude. This is particularly marked for the April flights where low values of $j(NO_2)$ were observed at low altitudes, leading to high values of NO_{Xcomp} and low values of the NO/NO_2 ratio. Interestingly, the amount of NO_X required for net photochemical production of O_3 to occur is considerably smaller at the higher altitudes than near the surface, largely because more of the NO_X is partitioned into NO.

4.2. Ozone Photochemical Production Rates

[32] During the flights in April, NO concentrations were measured and then used to constrain the model such that gross in situ O_3 photochemical production (P_{O3}) and loss (L_{O3}) rates were calculated along with the net in situ O_3

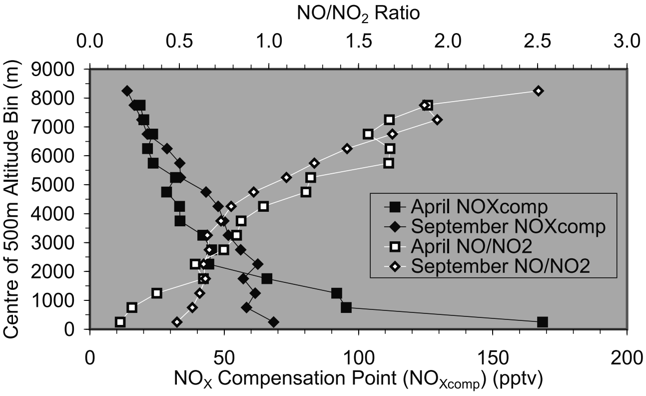

Figure 6. Mean NO_{Xcomp} values (black symbols) and mean NO/NO_2 ratios (white symbols) calculated for 500 m altitude bins for the April (squares) and September (diamonds) flights.

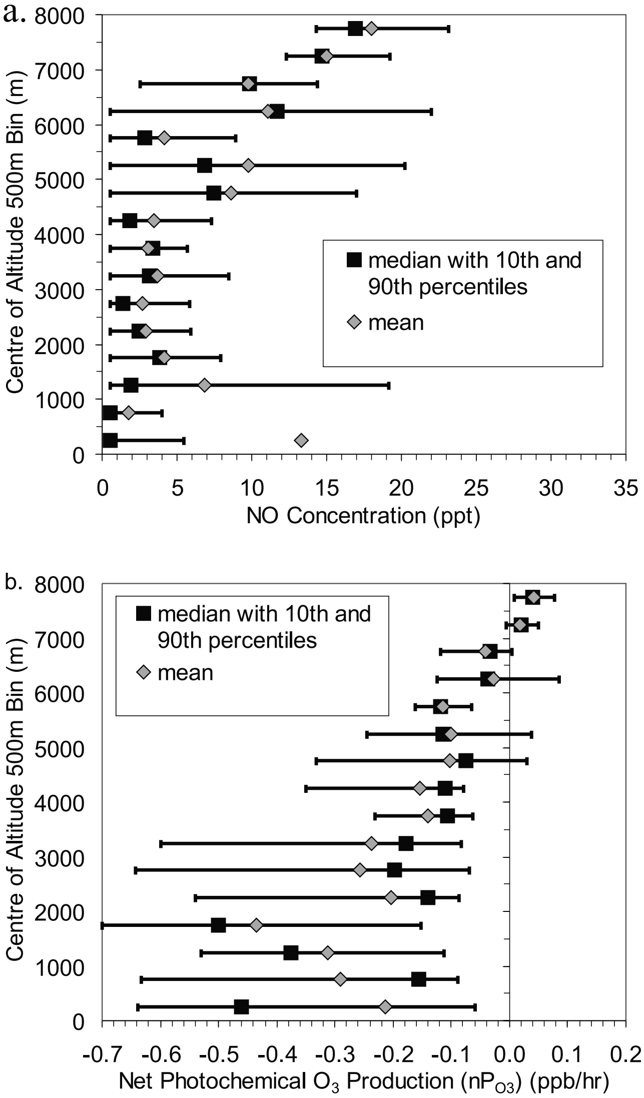

Figure 7. Mean (gray diamonds), median (black squares), 10th and 90th percentile (black bars) values for 500 m altitude bins for the April flights: (a) observed NO concentrations and (b) nP_{O3} rates.

photochemical production rates (nP_{O3}). Where the observed NO concentrations exceeded the calculated NO_{comp}, nP_{O3} was positive and vice versa.

[33] The average NO concentrations for each 500 m altitude bin during the spring flights were below 20 pptv (Figure 7a). The median values tended to increase with altitude from values of less than 5 pptv in the MBL to greater than 14 pptv above 7 km. On the other hand the mean values show more of a "C" shaped curve, illustrating that, on a few occasions, the lower altitude layers experienced much higher NO concentrations. One such incident is described in more detail below in the section 4.3.1.

[34] On average the NO concentrations (Figure 7a) were below the calculated values of NO_{comp} (Figure 2) for all altitudes below 7 km, giving negative values of nP_{O3} (Figure 7b) mostly between about −0.1 and −0.5 ppbv hr^{-1}. The trend of negative values of nP_{O3} decreasing in magnitude and switching to positive values with increasing altitude is a function of the values of NO_{comp} being lower at the higher altitudes, while the NO concentrations increased with altitude. The average calculated HO_2 mixing ratios are reasonably constant with altitude, while the average calculated CH_3O_2 decrease with altitude (Figure 3). As mentioned above in section 4.1, the rates of the reactions of the peroxy radicals with NO will increase slightly with altitude due to the decreasing temperature. However, the factor that changes the most with altitude is the NO concentration. It leads to an increase in P_{O3} with altitude, despite the decreasing effect of the reduced air density, such that on average it exceeds L_{O3} above 7 km (Figure 4).

[35] This trend in nP_{O3} is similar to that found by *Davis et al.* [1996] for the Pacific where nP_{O3} was negative below 6 km and slightly positive above 6 km. *Kotchenruther et al.* [2001] also found weak O_3 destruction for the remote springtime NE Pacific, with the net rate of destruction decreasing with altitude. *Yienger et al.* [1999] calculated nP_{O3} for 30°–60°N, in April at 685 mb and 500 mb and found it to be close to zero as the system switched from a winter regime of net O_3 production to a summer regime of net destruction.

[36] Although nP_{O3} showed this general trend with altitude, there were also a number of occasions where it varied from this, some of which are discussed in the case studies below (section 4.3).

4.3. Case Studies

4.3.1. MBL Including a Polluted Plume and Lower Free Tropospheric Air

[37] During flight A576 on 16 September 1997, air was sampled close to the ocean surface (down to 15 m altitude) off the coast of west Africa at about 29°W, 25°N (case 1, Table 2). Below about 2 km altitude the O_3 concentrations were mostly between 10 and 20 ppbv, while the H_2O concentrations were above 10,000 ppmv and even as high as 25,000 ppmv below 500 m altitude (Figure 8a). Back trajectories suggest that this air mass had remained over the ocean within 2 km of the surface for at least the previous 5 days. The photochemical lifetime of O_3 is calculated to be 5 days given the conditions observed and assuming these conditions had been similar for the previous few days, this would explain the low O_3 concentrations observed. Dry deposition is also likely to have contributed to the loss of this O_3. These conditions, in particular the low O_3 concentrations, lead to a low NO_{comp} value of around 20 pptv. Therefore the moist MBL has provided an environment where O_3 loss has occurred to such an extent that only a small amount of NO is required to switch the system back into one of nP_{O3}. In a remote oceanic region this NO might come from ship emissions [*Lawrence and Crutzen*, 1999; *Kasibhatla et al.*, 2000], or possibly from the thermal decomposition of PAN as the air subsides from the free troposphere [*Moxim et al.*, 1996].

[38] Similar conditions were encountered during flight A575 on 14 September 1997, when air was sampled close to the ocean surface (down to 15 m altitude) at about 25°W, 31°N (case 2, Table 2). Below about 1 km altitude the O_3 concentrations were mostly between 18 and 30 ppbv, while the H_2O concentrations were above 16,000 ppmv and even as high as 28,000 ppmv near the surface (Figure 8b). Back trajectories suggest that the air mass had come from over west Africa, passing over the ocean for at least the previous

Table 2. Summary of Case Studies

No.	Flight	Date (dd.mm.yy)	Time (hhmm)	Altitude (km)	H_2O (ppmv)	O_3 (ppbv)	NO_{comp} (pptv)	NO (pptv)	nP_{O3} (ppbv hr $^{-1}$)
1	A576	16.09.97	1553–1635	<2	10,000–25,000	10–20	16	NA	NA
2	A575	14.09.97	1426–1455	<1	15,000–28,000	18–30	24	NA	NA
3a[a]	A575	14.09.97	1711–1726	<1	18,000–28,000	33–43	24	NA	NA
3b[a]	A575	14.09.97	1711–1726	<1	18,000–28,000	33–43	33	NA	NA
4	A576	16.09.97	1407, 1439	3	9000–1000	60	>50	NA	NA
5	A534	07.04.97	1417	0.25	15,300	46	30	278	3.1
6	A579	20.09.97	1500–1529	6–8	500	33	10	NA	NA
7	A576	16.09.97	1531–1536	6	800	82	24	NA	NA
8	A533	05.04.97	1030–1330[b]	6	200–600	57	12	10–30	<0.15
9	A533	05.04.97	1103–1127	6	1400	46	12	<10	−0.05
10a	A536	10.04.97	1100–1135, 1200–1218, 1236–1258	5.2	2300	57	20	<5	−(0.15–0.30)
10b	A536	10.04.97	1225, 1317	6.4, 5.2	980, 1130	66, 70	16, 17	25	<0.1
10c	A536	10.04.97	1145–1147	5.2	360	79	17	>60	0.4

[a] The photolysis rates in 3b are the average of those during case 2 (see text for more details).
[b] Excluding case 9.

3 days during which it had remained within 2 km of the surface. Again this could explain the low O_3 concentrations observed and the relatively low NO_{comp} values calculated (21–26 pptv).

[39] However, 2-1/2 hours later at 36°W, 31°N the aircraft again sampled MBL air with very similar H_2O concentrations, but this time the O_3 concentrations were higher (between 33 and 41 ppbv) (case 3a, Table 2) (Figure 8c). The back trajectories suggest that the air had descended from altitudes of between 1 and 8 km during the last 6 days and may only have been within the MBL for the last couple of days. Therefore, since the O_3 had been subjected to the high photochemical losses associated with the moist MBL for a shorter period, this might explain why the O_3 concentrations were higher. The calculated NO_{comp} values are 23–27 pptv, similar to those in case 2, despite the higher O_3 concentrations. However, it should noted that case 3a is much later in the day when the solar zenith angle would have been much higher and photolysis rates, in particular that of $j(O(^1D))$, much lower. In case 3b, the model was run with the photolysis rates set at the mean of those during the period of case 2 (i.e., $j(O(^1D))$ and $j(NO_2)$ increased by factors of 2.0 and 1.2, respectively). NO_{comp} for case 3b are 31–34 pptv. Comparison of the NO_{comp} values calculated for cases 2, 3a, and 3b, illustrate that both higher O_3 concentrations and higher photolysis rates (lower

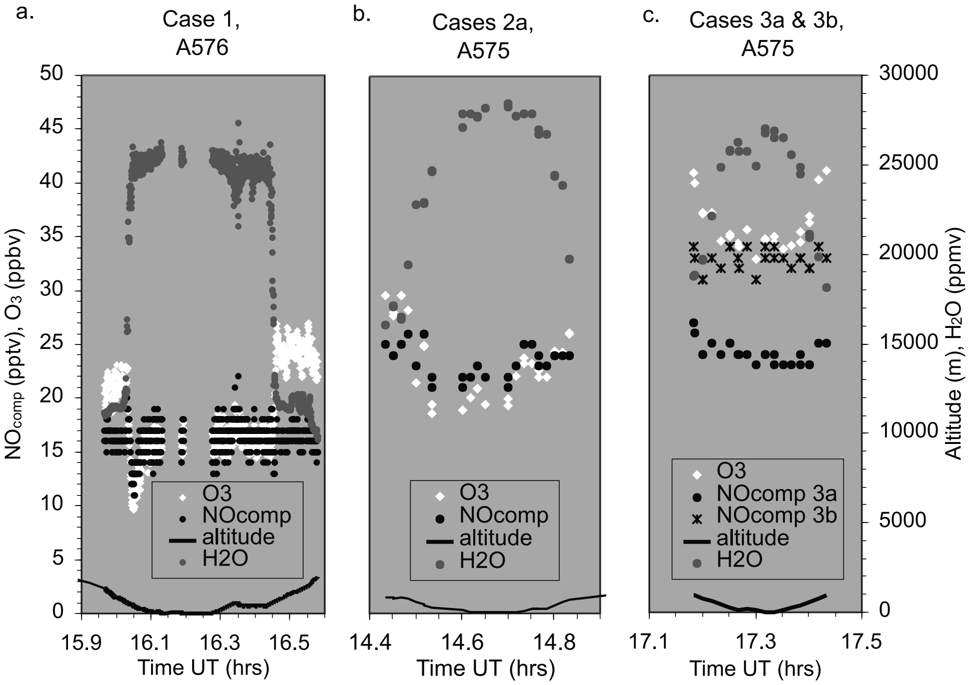

Figure 8. Time series of observed H_2O (gray dots) and O_3 (white diamonds) concentrations, altitude (black line) and calculated values of NO_{comp} (black dots, with black asterisks for case 3b): (a) case 1 (flight A576 on 16 September 1997), (b) case 2 (flight A575 on 14 September 1997), and (c) cases 3a and 3b (flight A575 on 14 September 1997).

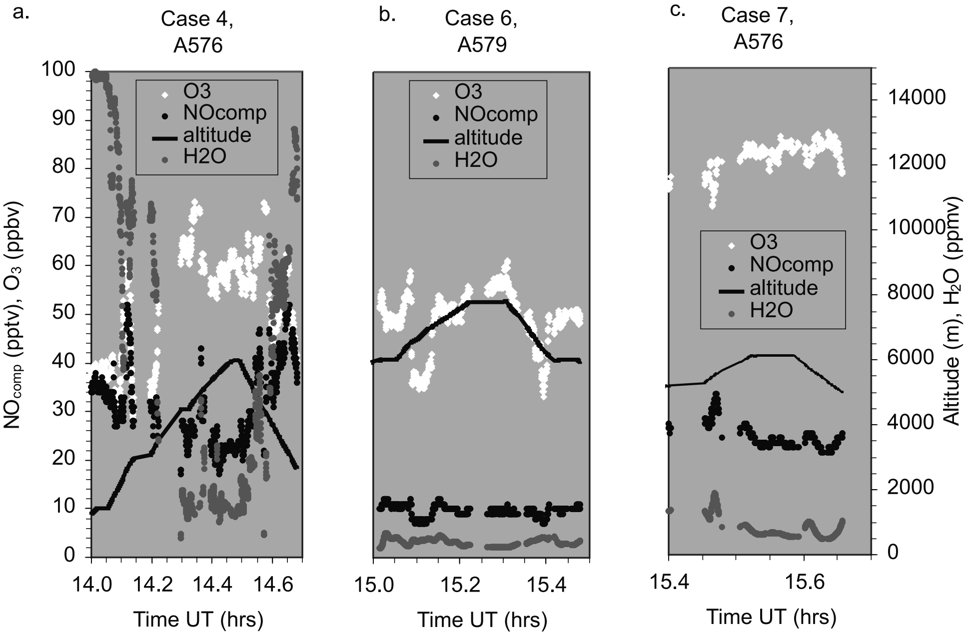

Figure 9. Time series of observed H_2O (gray dots) and O_3 (white diamonds) concentrations, altitude (black line) and calculated values of NO_{comp} (black dots): (a) case 4 (flight A576 on 16 September 1997), (b) case 6 (flight A579 on 20 September 1997), and (c) case 7 (flight A576 on 16 September 1997).

zenith angles) lead to higher values of NO_{comp}. It is interesting to note that while NO_{comp} increased by about 40% between cases 3a and 3b, NO_{Xcomp} only increased by about 30%. Effectively, higher photolysis rates associated with lower solar zenith angles shifts the internal partitioning of NO_X toward NO, requiring relatively less NO_X to support the amount of NO needed for net photochemical production of O_3.

[40] The highest NO_{comp} values were calculated for air at about 3 km altitude during flight A576 on 16 September 1997 (case 4, Table 2) (Figures 9a and 5b). This air was intersected on a number of occasions as the aircraft profiled southward from the Azores and then again on the return northward. The H_2O concentrations were high in the MBL and gradually decreased with altitude. The O_3 concentrations were low in the MBL and exhibited a rapid increase at about 2–3 km. This gave rise to a layer of air with both moderate O_3 and H_2O concentrations (60 ppbv and 9000–10,000 ppmv, respectively), which together resulted in calculated values of NO_{comp} up to 50 pptv. Back trajectories suggest that this had come from the west and had remained at about 3 km altitude for the previous 6 days.

[41] During flight A534 on 7 September 1997 the aircraft descended from an altitude of 8 km to close to the ocean surface at about 43°N, 39°W (Figure 10). During the descent H_2O concentrations increased, O_3 concentrations decreased, with the net effect of an increase in L_{O3} to about 0.6 ppbv hr^{-1} and an increase in NO_{comp} (Figure 10c). NO concentrations decreased to below detection limit (<1 pptv), such that P_{O3} was very small and nP_{O3} switched from being slightly positive above about 7 km to being negative below. However, a plume with high concentrations of NO (>250 pptv) was observed (case 5, Table 2) in a decoupled layer within the MBL. The origin of this NO is believed to be ship emissions as discussed in more detail by *Bauguitte* [2000]. The O_3 production calculated for this plume is far in excess of the O_3 loss, despite the high H_2O concentrations (15,000 ppmv), leading to large positive values of nP_{O3} (3 ppbv hr^{-1}) (Figure 10b). This illustrates a situation where an in situ source of NO in the remote marine atmosphere has led to a considerable enhancement in local concentrations of NO_X along with net O_3 production, albeit in a narrow plume (150 m depth). Such observations contribute to recent discussions concerning the influence of shipping emissions on the chemistry of the remote MBL [*Lawrence and Crutzen*, 1999; *Kasibhatla et al.*, 2000].

[42] These case studies illustrate that the value of NO_{comp} in the MBL can largely be a function of the time that the air mass has been within the MBL and subject to high H_2O concentrations. The resulting low O_3 concentrations can give rise to low values of NO_{comp}, which would explain why there is often not a simple relationship of decreasing NO_{comp} with increasing altitude in the lower troposphere. Further, an example is given where an in situ source of NO_X led to high net O_3 production rates in the remote MBL.

4.3.2. Middle and Upper Tropospheric Air

[43] Flight A579 on 20 September 1997, illustrates how uplifted air can affect the potential for net O_3 production in the middle and upper troposphere (case 6, Table 2). Between 6 and 8 km at the top of the profile just after 1500 UT (Universal Time), the H_2O concentrations were very low (about 500 ppmv), while the O_3 concentrations were variable, as low as 33 ppbv, but averaging about 50 ppbv (Figure 9b). Back trajectories suggest that this air had been lifted up from near the surface over the Pacific 4–6 days before. Some of this air appears to have risen up to 8–9 km before descending back down to 6–7 km. Condensation nuclei concentrations were elevated in this air mass while CO concentrations were suppressed. This is indicative of convectively uplifted MBL [*Ridley et al.*, 1997]. In this case the air was very dry, presumably due to the air being

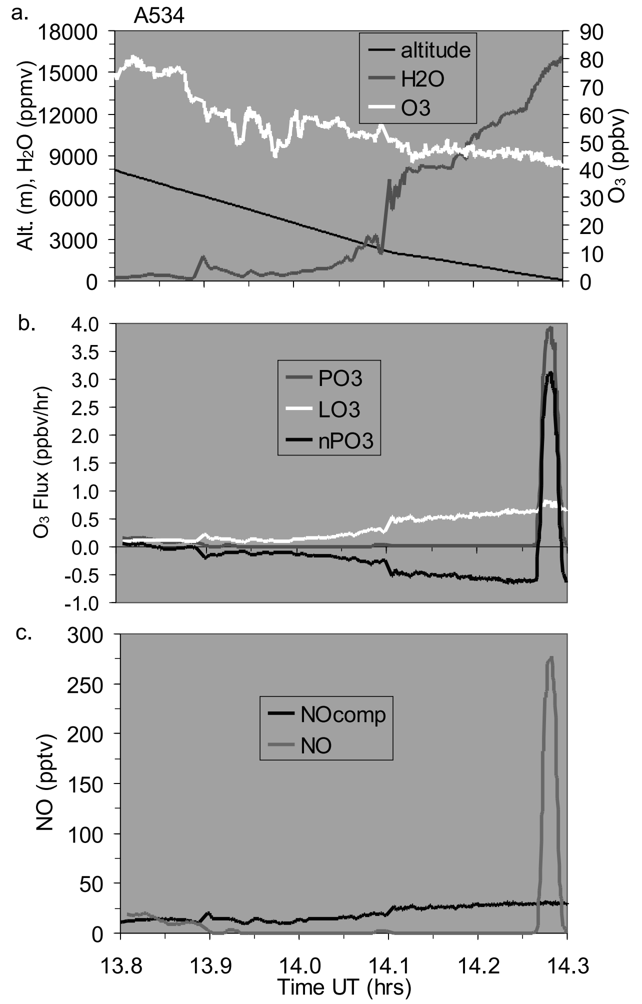

Figure 10. Times series for case 5 (flight A534 on 7 April 1997): (a) observed H_2O (gray line) and O_3 (white line) concentrations and altitude (black line), (b) calculated values of L_{O3} (white line), P_{O3} (gray line), and nP_{O3} (black line), and (c) observed concentrations of NO (gray line) and calculated values of NO_{comp} (black line).

cooled during uplift, becoming saturated and the water being removed through precipitation. Consequently, air in the middle and upper troposphere was found to have O_3 concentrations perhaps more typical of the lower troposphere, while having low H_2O concentrations. This led to very low calculated NO_{comp} values of around 10 pptv.

[44] In contrast, air at 6 km altitude was sampled at 29°W, 27°N during flight A576 on 16 September 1997 (case 7, Table 2). On this occasion, the O_3 concentrations were much higher at about 82 ppbv, with H_2O concentrations again low at about 800 ppmv (Figure 9c). This time the back trajectories suggest that the air had remained at high altitudes for the last 10 days, if anything it had descended a couple of kilometers. This would suggest that low water concentrations had persisted for several days and with an O_3 lifetime of the order of 50 days in these conditions, this might explain why the air contained much higher O_3 concentrations. Furthermore relatively high concentrations of CO (100 ppbv) were observed in this air mass, indicating that the air contained anthropogenic O_3 precursors. The 10-day back trajectories extend back over the US. It is possibly that convection, unresolved by the trajectory calculations, lifted up polluted air over the US to an altitude of 8 km or more, during which the air cooled and was dried. O_3 may have been photochemically produced or possibly mixed in from surrounding upper tropospheric air and then transported to the eastern side of the North Atlantic, similar to that described by *Wild et al.* [1996] and *Stohl and Trickl* [1999]. Even though the air was fairly dry, the calculated NO_{comp} values were relatively high (21–33 pptv), largely because of the higher O_3 concentrations.

[45] In transit from the UK to the Azores (Flight A533) on 5 April 1997, the aircraft flew at 6 km altitude, during most of which the H_2O concentrations were between 200 and 600 ppmv and O_3 concentrations averaged 57 ppbv (Figure 11a). In these dry conditions and moderate O_3 concentrations, O_3 loss was calculated to be low (mostly <0.15 ppbv hr^{-1}) (Figure 11b) and consequently on average

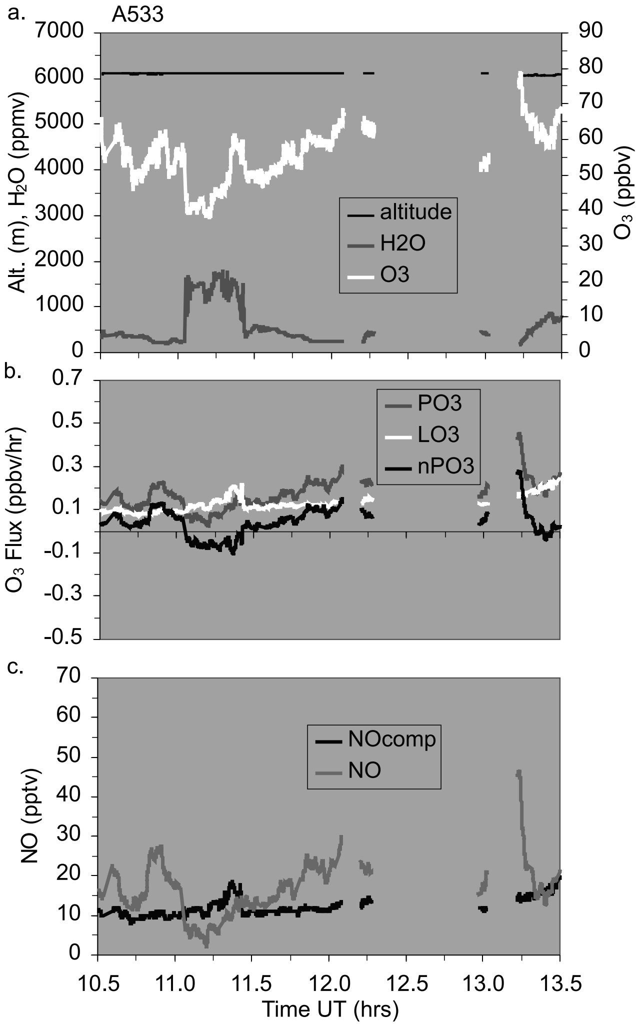

Figure 11. Times series for cases 8 and 9 (flight A533 on 5 April 1997): (a) observed H_2O (gray line) and O_3 (white line) concentrations and altitude (black line), (b) calculated values of L_{O3} (white line), P_{O3} (gray line), and nP_{O3} (black line), and (c) observed concentrations of NO (gray line) and calculated values of NO_{comp} (black line).

(excluding 1103–1127 UT) NO_{comp} was calculated to be 12 pptv (Figure 11c) (case 8, Table 2). Reaction with HO_2 was the dominant calculated loss path for O_3 (~60%). Throughout this time, NO concentrations were observed to be above the NO_{comp} values (Figure 11c), such that the nP_{O3} values were calculated to be positive, but small (mostly <0.15 ppbv hr^{-1}) (Figure 11b). Between 1103 and 1127 UT when the back trajectories suggest that the air had been lifted up from the MBL over the North Atlantic, H_2O concentrations were slightly higher (1400 ppmv), O_3 concentrations were lower (46 ppbv) (case 9, Table 2) and photolysis of O_3 was calculated to be its major loss path (~40%). During this period NO_{comp} averaged 12 pptv, rising to 18 pptv for a short time, toward the end as O_3 concentrations rose. Furthermore, the observed NO concentrations in this uplifted MBL air were lower, such that they were below NO_{comp} and the nP_{O3} values were calculated to be negative (-0.05 ppbv hr^{-1}). For this particular flight most of the free tropospheric air at 6 km altitude was calculated to have small positive net O_3 production rates. It was at 6 km altitude that *Davis et al.* [1996] noted a switch between negative net O_3 production rates below and small positive values above. The current results are consistent with this, but also illustrate how uplifted MBL air with both higher NO_{comp} values and lower NO concentrations can affect O_3 production rates of the free troposphere.

[46] Five days later, on 10 April 1997, the aircraft returned from the Azores to the UK (Flight A536) and during the transit remained at just above 5.2 km altitude for most of the time (Figure 12a), although it did fly at 6.4 km for a brief period of about 20 min. In comparison to flight A533, the H_2O concentrations were on average higher (1500 ppmv), similar to those of the uplifted MBL air, although there were periods when drier air was observed. These included the time when the aircraft flew at the higher altitude and for about 25 min just after 1135 UT. On average the O_3 concentrations (63 ppbv) were higher than during the transit run of flight A533. The higher H_2O and O_3 concentrations combined to produce higher loss rates of O_3 (average L_{O3} = 0.21 ppbv hr^{-1}) (Figure 12b). NO_{comp} for A536 is calculated to be higher (18 pptv) than for A533, due to the larger photochemical loss, which, for the most part, is not exceeded by P_{O3}. That is, nP_{O3} was mostly negative, again similar to the findings of *Davis et al.* [1996] for PEM-West A. The differences between the 2 flights may partly be a result of the generally lower altitude (5.2 km) at which the aircraft flew on the return leg (A536), with the air observed at 6.4 km altitude during A536 being more typical of the air sampled on A533. However, air masses with differing chemical characteristics were observed at the same altitude, a result of their different origins and histories.

[47] H_2O was found to be negatively correlated to O_3. The calculated L_{O3} is largely well correlated to H_2O (although partly moderated by the O_3), such that NO_{comp} is higher in the moister air (Figure 12). Photolysis of O_3 is the major calculated loss (50%) in the moister air, while reaction with HO_2 is the largest calculated loss (55%) in the drier air. The peroxy radicals are a product of the photolytic O_3 loss so are closely correlated with H_2O and L_{O3} and in this case tend to be negatively correlated to the NO (Figure 12). The peroxy radicals ($HO_2 + CH_3O_2$) vary from 20 to 30 pptv although it should be noted that, for this flight, the CO and CH_4 concentrations are held constant. Grab samples suggest that the CO concentrations were slightly elevated at times (150 ppbv, 1130–1200 UT; 140 ppbv, 1315–1500 UT) and slightly lower at others (115 ppbv, 1200–1300 UT). Given this caveat, it is the variation in the NO that is largest, varying from below detection limit (1 pptv) to 25 or even 65 pptv (Figure 12c) and consequently P_{O3} is strongly correlated to the NO concentrations and is greater in the dry air where L_{O3} is less. With P_{O3} and L_{O3} being negatively correlated, the nP_{O3} follows a similar pattern to P_{O3} but with an even larger variation between different air masses (Figure 12b).

[48] In the moister air the NO concentrations were very low (<5 pptv) and nP_{O3} is mostly -0.15 to -0.3 ppbv hr^{-1} (case 10a, Table 2). However, in 3 cases where drier air was sampled the NO concentrations exceeded NO_{comp} such that nP_{O3} is positive. It is only slightly positive (<0.1 ppbv hr^{-1}) in 2 of these cases (case 10b, Table 2), but in the dry air sampled at 1145 UT the NO concentrations exceeded 60 pptv and nP_{O3} was calculated to reach 0.4 ppbv hr^{-1} (case 10c, Table 2). Interestingly the observed O_3 is lowest where nP_{O3} is negative and highest where nP_{O3} is positive, consistent with the O_3 concentrations being controlled, to some extent, by in situ photochemistry.

[49] Back trajectories for the dry air sampled at 1145 UT suggest that 6 days before it was at 5–10 km altitude over the eastern Pacific and crossed North America in the middle to upper troposphere, descending to 5 km over the Atlantic. This air mass contained 65 pptv of NO so it had clearly been influenced by sources of pollution, but it is not clear where this had come from. Since the trajectories remained in the middle to upper troposphere, it might be that the pollution came from Asia. However, the trajectories do not take account of convection, which may have lifted up polluted boundary layer air from over North America. This particular incident of long-range transport in which air with positive net O_3 production rates was observed over the eastern North Atlantic is discussed in more detail by *Bauguitte* [2000]. The air mass observed just prior to 1130 UT was lifted up from the North Atlantic MBL, hence its higher H_2O concentrations. After 1200 UT the back trajectories suggest a variety of air masses were observed from over the mid-Atlantic, Africa, and western Europe.

5. Sensitivity Tests

5.1. Photolysis Rates

[50] To examine the sensitivity of the model results to the assumed ratio between $j(O(^1D))$ and $j(NO_2)$, the model was run for the spring flights with this ratio, first increased by 30% and second decreased by 30%. The effect is examined in terms of changes to the median values obtained for each 500 m altitude bin. Increasing (decreasing) $j(O^1D))$ by 30% has the effect of increasing (decreasing) the loss of O_3 through reaction of $O(^1D)$ with H_2O by 30%. The fluxes through the reactions of HO_2 and OH are increased (and decreased), but by not as much. The HO_2 flux is altered by about 13% near the surface, but this change decreases to only 3% above 7 km altitude. Similarly, the OH flux is altered by about 25% near the surface, with this change decreasing to only 7% above 7 km altitude. This decrease in the effect with altitude of $j(O(^1D)$ on these fluxes reflects

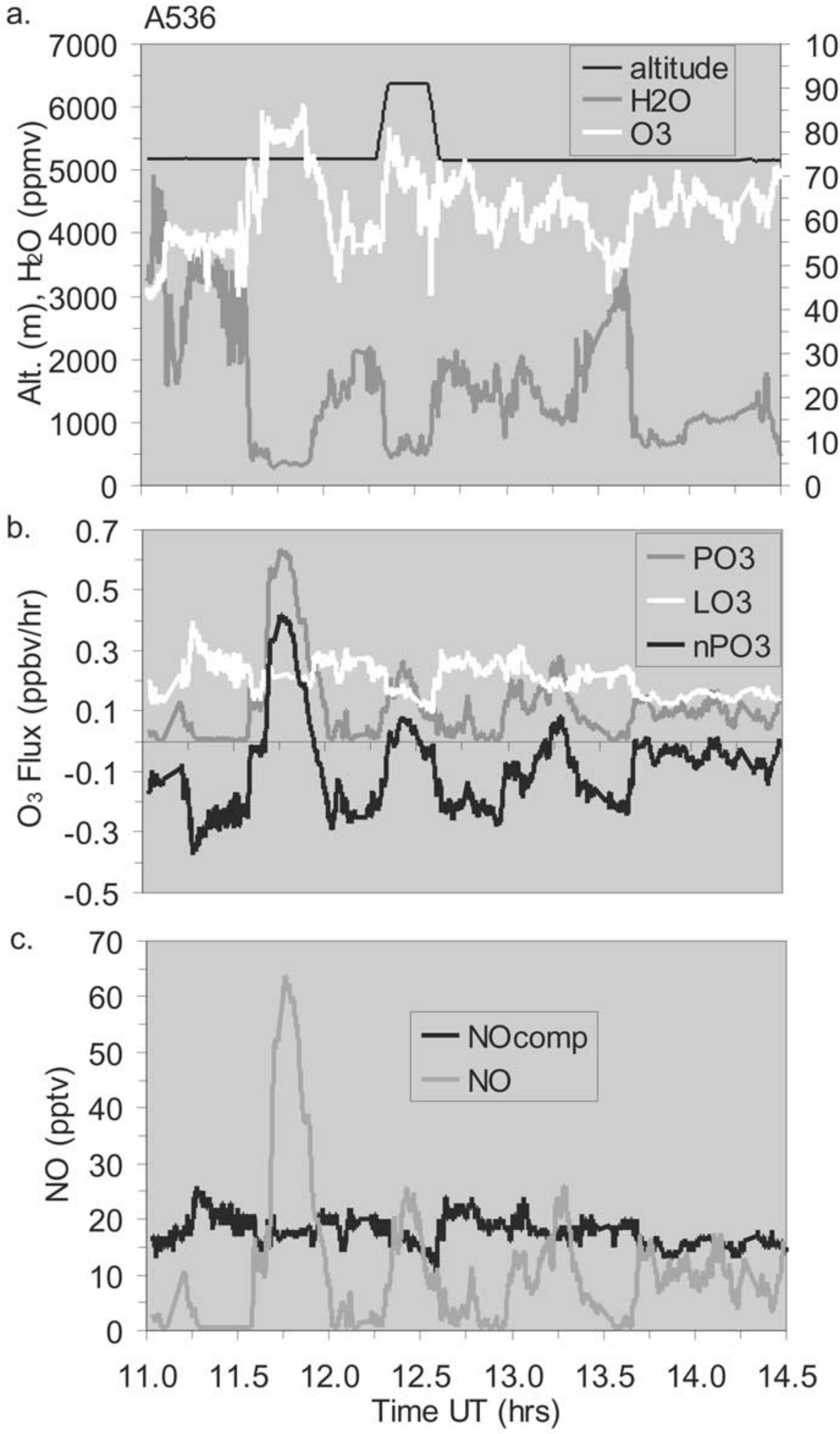

Figure 12. Times series for cases 10a, 10b, and 10c (flight A536 on 10 April 1997): (a) observed H_2O (gray line) and O_3 (white line) concentrations and altitude (black line), (b) calculated values of L_{O3} (white line), P_{O3} (gray line), and nP_{O3} (black line), and (c) observed concentrations of NO (gray line) and calculated values of NO_{comp} (black line).

the decrease in importance of the photolysis of O_3 as a source of these radicals. The overall effect on L_{O3} is for it to increase (decrease) by about 20–25% below about 2.5 km, with this change decreasing to only 8% above 7 km altitude. NO_{comp} increases (decreases) by about 2 pptv below about 6 km. However, above 7 km this change is less than 1 pptv. P_{O3} increases (decreases) due to the effect of the changed $j(O(^1D))$ on the peroxy radicals. The magnitude of this change in P_{O3} is similar to that of the HO_2 concentrations (13% near the surface, decreasing to 3% above 7 km altitude). The changes in P_{O3} and L_{O3} are both in the same direction, but since the actual change in L_{O3} is larger, the increase (decrease) in $j(O(^1D)$ brings about a shift toward more negative (positive) values of nP_{O3}. This shift is of about 0.1 ppbv hr^{-1} near the surface, decreasing to only 0.005 ppbv hr^{-1} above 7 km. The altitude of the switch from negative values to positive values of nP_{O3} remains at 7 km.

5.2. NO Concentrations

[51] *Peterson et al.* [1998] made measurements of NO on the Azores during August and September 1993 at an altitude of 1 km and found a free tropospheric solar noontime mean of 17.1 pptv and median of 15.7 pptv. These averages are higher than observed during the ACSOE flights in April between 0900 and 1800 UT, which, below 4.5 km, were mostly below 5 pptv, often below detection limit (1 pptv) and rarely exceeded 15 pptv. These average results are dependent on the air masses sampled during the 3 spring flights, which for many of these bins were often maritime in origin, based on 6-day back trajectories. One area of uncertainty in the measurement of NO is the artifact of between 5 and 8 pptv (see section 2), which becomes very significant at the low concentrations observed. As a sensitivity test, the observed NO concentrations were recalculated without accounting for the artifact and then new O_3 production rates were calculated. Without removing the artifact the NO concentrations are clearly higher, with the 10th percentile values also showing the general increase with altitude (Figure 13a). Further the altitude above which the NO concentrations tend to exceed NO_{comp}, giving positive values of nP_{O3}, is lowered from 7 to 6 km (Figure 13b). Although photochemical production of O_3 is increased at all altitudes, nP_{O3} is only increased by about 0.07 ppbv hr^{-1} such that below 6 km net photochemical loss is still calculated to occur. Therefore the uncertainty in the artifact does not change the general conclusion reached above that slow net photochemical O_3 loss occurred in the lower and mid troposphere with slow nP_{O3} in the upper troposphere.

6. Summary

[52] On average NO_{comp} showed no clear correlation with altitude in the lowest 4 km of the atmosphere with values mostly between 15 and 25 pptv, but above this height it decreased with increasing altitude to 10–15 pptv at 6–8 km. At the higher altitudes, it was the lower H_2O concentrations that led to less O_3 loss and hence lower values for NO_{comp}. NO_{Xcomp} showed a clear decrease with altitude due to the additional effect of the increase in $j(NO_2)$ which shifts the internal partitioning of NO_X toward NO thus requiring less NO_X to support the amount of NO needed for net photochemical production of O_3 to occur.

[53] Some of the variation in the value of NO_{comp} in the MBL appeared to be attributed to the length of time the air had been subject to the moist, photochemically active conditions. O_3 concentrations and calculated values of NO_{comp} were often found to be low in air which appeared to have been within the moist MBL for several days, while MBL air with both higher O_3 concentrations and values of NO_{comp} appeared to be associated with air which had recently descended from the free troposphere. This suggests that the moist MBL provides an environment for rapid O_3 loss, but in which, once O_3 has been substantially depleted, only a small amount of NO is required to switch the system back into one of nP_{O3}.

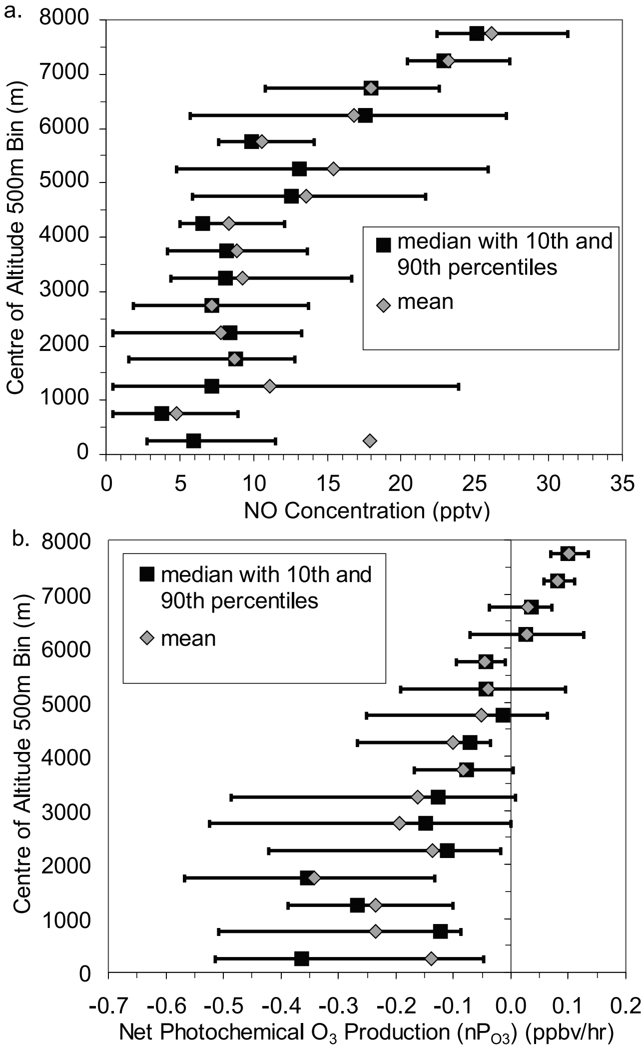

Figure 13. Mean (gray diamonds), median (black squares), 10th and 90th percentile (black bars) values for 500 m altitude bins for the April flights: (a) observed NO concentrations with no artifact removed and (b) nP_{O3} rates calculated using NO with no artifacts removed.

[54] The values of NO_{comp} calculated for air masses in the middle and upper troposphere varied greatly depending on the H_2O and O_3 concentrations. Air masses at the same altitude had very different concentrations of H_2O and O_3, which could be attributed to their differing origins and histories. Air with low O_3 concentrations, which appeared to have been lifted up from the lower troposphere had much lower values of NO_{comp} than air, with higher O_3 concentrations, which was possibly polluted and had recently descended from the upper troposphere. The highest values of NO_{comp} were calculated for lower tropospheric air where both H_2O and O_3 concentrations were reasonably high.

[55] The calculated photochemical O_3 production rates were mostly negative in the air masses sampled in April and generally went from being about -0.5 to -0.2 ppbv hr^{-1} in

the MBL to +0.04 ppbv hr^{-1} at about 7–8 km altitude. This vertical trend in nP_{O3} was largely because at the higher altitudes NO_{comp} was lower, while the NO concentrations were generally higher thus increasing O_3 production. Although nP_{O3} showed this general trend with altitude, there were a number of occasions where it varied from this for example in cases where NO_{comp} did not show a negative correlation with altitude and also in a case where a plume with high NO concentrations was observed just above the MBL.

[56] The nP_{O3} rates calculated for air masses observed between 5 and 6.5 km during the spring were found to be both negative and positive. In these air masses the loss of O_3 was largely correlated to H_2O, but was also moderated by the O_3, such that NO_{comp} tended to be higher in the moister air. However, the observed NO concentrations were negatively correlated to the H_2O. Since the production of O_3 was strongly correlated to the NO concentrations and was greater in the dry air where O_3 loss was less, the nP_{O3} rates followed a similar pattern with positive values in the drier air masses and negative values in the moister air masses.

[57] This work suggests that the much of the lower and middle troposphere over the eastern North Atlantic during spring is in a state of slow net photochemical O_3 destruction. However, in the upper troposphere, the system changes to one of net photochemical production, which results from the drier environment and higher NO concentrations. Furthermore, examples of net O_3 production were also observed in the lower and middle troposphere either associated with in situ sources of NO or long-range transport of pollution. This work also illustrates the sensitivity of this O_3 production/loss state to H_2O and NO concentrations, photolysis rates and temperatures.

[58] **Acknowledgments.** The authors wish to thank the Natural Environment Research Council for funding the Atmospheric Chemistry Studies of the Oceanic Environment (ACSOE) program. This paper is number ACP168 in the ACSOE series. We also wish to acknowledge those of the UK Meteorological Research Flight and Royal Air Force who made the aircraft flight campaign possible, the British Atmospheric Data Centre for data support, the UK Meteorological Office and European Centre for Medium-Range Weather Forecast for provision of analysis data for trajectory calculations, and the NASA/Goddard Space Flight Center for TOMS data. Claire Reeves would also like to recognize the National Center for Atmospheric Research (NCAR) for support during a visit in which much of the model development was done.

References

Bauguitte, S., A study of tropospheric reactive nitrogen oxides in the North Atlantic region, Ph.D. thesis, Univ. of East Anglia, Norwich, UK, 2000.

Carpenter, L. J., P. S. Monks, B. J. Bandy, S. A. Penkett, I. E. Galbally, and C. P. Meyer, A study of peroxy radicals and ozone photochemistry at coastal sites in the Northern and Southern Hemispheres, *J. Geophys. Res.*, *102*, 25,417–25,427, 1997.

Carpenter, L. J., T. J. Green, G. P. Mills, S. Bauguitte, S. A. Penkett, P. Zanis, E. Schuepbach, N. Schmidbauer, P. S. Monks, and C. Zellweger, Oxidized nitrogen and ozone production efficiencies in the springtime free troposphere over the Alps, *J. Geophys. Res.*, *105*, 14,547–14,559, 2000.

Cox, R. A., Ozone and peroxy radical budgets in the marine boundary layer: Modelling the effect of NO_X, *J. Geophys. Res.*, *104*, 8047–8056, 1999.

Davis, D. D., et al., Assessment of ozone photochemistry in the western North Pacific as inferred from PEM-West A observations during fall 1991, *J. Geophys. Res.*, *101*, 2111–2134, 1996.

DeMore, W. B., S. P. Sander, C. J. Howard, A. R. Ravishankara, D. M. Golden, C. E. Kolb, R. F. Hampson, M. J. Kurylo, and M. J. Molina, Chemical kinetics and photochemical data for use in stratospheric modelling: Evaluation number 12, *JPL Publ.*, *97-4*, 14–143, 1997.

Edwards, G. D., Aircraft studies of atmospheric chemistry over the North Atlantic, Ph.D. thesis, Univ. of Leicester, Leicester, UK, 2000.

Frost, G. J., et al., Comparisons of box model calculations and measurements of formaldehyde from the 1997 North Atlantic Regional Experiment, *J. Geophys. Res.*, *107*(D12), 4060, doi:10.1029/2001JD000896, 2002.

Gerbig, C., S. Schmitgen, D. Kley, A. Volz-Thomas, K. Dewey, and D. Haaks, An improved fast-response vacuum-UV resonance fluorescence CO instrument, *J. Geophys. Res.*, *104*, 1699–1704, 1999.

Kasibhatla, P., et al., Do emissions from ships have a significant impact on concentrations of nitrogen oxides in the marine boundary layer?, *Geophys. Res. Lett.*, *27*, 2229–2232, 2000.

Klonecki, A., and H. Levy II, Tropospheric chemical ozone tendencies in the $CO-CH_4-NO_Y-H_2O$ system: Their sensitivity to variations in environmental parameters and their application to a global chemistry transport model story, *J. Geophys. Res.*, *102*, 21,221–21,237, 1997.

Kotchenruther, R. A., D. A. Jaffe, and L. Jaeglé, Ozone photochemistry and the role of peroxyacetyl nitrate in the springtime northeastern Pacific troposphere: Results from the Photochemical Ozone Budget of the Eastern North Pacific Atmosphere (PHOBEA) campaign, *J. Geophys. Res.*, *106*, 28,731–28,742, 2001.

Lawrence, M. G., and P. J. Crutzen, Influence of NO_x emissions from ships on tropospheric photochemistry and climate, *Nature*, *402*, 167–170, 1999.

Levy, H., II, Normal atmosphere: Large radical and formaldehyde concentrations predicted, *Science*, *173*, 141–143, 1971.

Madronich, S., and S. Flocke, The role of solar radiation in atmospheric chemistry, in *Handbook of Environmental Chemistry*, edited by P. Boule, pp. 1–26, Springer-Verlag, New York, 1998.

Moxim, W. J., H. Levy II, and P. S. Kasibhatla, Simulated global tropospheric PAN: Its transport and impact on NO_X, *J. Geophys. Res.*, *101*, 12,621–12,638, 1996.

Newell, R. E., Z.-X. Wu, Y. Zhu, W. Hu, E. V. Browell, G. L. Gregory, G. W. Sachse, J. E. Collins Jr., K. K. Kelly, and S. C. Liu, Vertical fine-scale atmospheric structure measured from NASA DC-8 during PEM-West A, *J. Geophys. Res.*, *101*, 1943–1960, 1996.

Penkett, S. A., B. J. Bandy, C. E. Reeves, D. McKenna, and P. Hignett, Measurements of peroxides in the atmosphere and their relevance to the understanding of global tropospheric chemistry, *Faraday Discuss.*, *100*, 155–174, 1995.

Penkett, S. A., C. E. Reeves, B. J. Bandy, J. M. Kent, and H. R. Richer, Comparison of calculated and measured peroxide data collected in marine air to investigate prominent features of the annual cycle in the troposphere, *J. Geophys. Res.*, *103*, 13,377–13,388, 1998.

Peterson, M. C., R. E. Honrath, D. D. Parrish, and S. J. Oltmans, Measurements of nitrogen oxides and a simple model of NO_Y fate in the remote North Atlantic marine atmosphere, *J. Geophys. Res.*, *103*, 13,489–13,504, 1998.

Ridley, B. A., E. L. Atlas, J. G. Walega, G. L. Kok, T. A. Staffelbach, J. P. Greenberg, F. E. Grahek, P. G. Hess, and D. D. Montzka, Aircraft measurements made during the spring maximum of ozone over Hawaii: Peroxides, CO, O_3, NO_y, condensation nuclei, selected hydrocarbons, halocarbons, and alkyl nitrates between 0.5 and 9 km altitude, *J. Geophys. Res.*, *102*, 18,935–18,961, 1997.

Sander, S. P., et al., Chemical kinetics and photochemical data for use in stratospheric modelling: Supplement to evaluation number 12: Evaluation number 13, *JPL Publ.*, *00-3*, 10–28, 2000.

Stohl, A., and T. Trickl, A textbook example of long range transport: Simultaneous observations of ozone maxima of stratospheric and North American origin in the free troposphere over Europe, *J. Geophys. Res.*, *104*, 30,445–30,462, 1999.

Volz-Thomas, A., A. Lerner, H. W. Patz, M. Schultz, D. S. McKenna, R. Schmitt, S. Madronich, and E. P. Roth, Airborne measurements of the photolysis of NO_2, *J. Geophys. Res.*, *101*, 18,613–18,627, 1996.

Wild, O., K. S. Law, D. S. McKenna, B. J. Bandy, S. A. Penkett, and J. A. Pyle, Photochemical trajectory modeling studies of the North Atlantic region during August 1993, *J. Geophys. Res.*, *101*, 29,269–29,288, 1996.

Yienger, J. J., A. A. Klonecki, H. Levy II, W. J. Moxim, and G. R. Carmichael, An evaluation of chemistry's role in the winter–spring ozone maximum found in the north midlatitude free troposphere, *J. Geophys. Res.*, *104*, 3655–3667, 1999.

B. J. Bandy, S. Bauguitte, S. A. Penkett, and C. E. Reeves, School of Environmental Sciences, University of East Anglia, Norwich, UK. (c.reeves@uea.ac.uk)

H. Barjat, K. Dewey, and J. Kent, Meteorological Research Flight, UK Meteorological Office, Farnborough, UK.

G. D. Edwards, P. S. Monks, and G. Phillips, School of Chemistry, University of Leicester, Leicester, UK.

M. J. Evans and K. S. Law, Centre for Atmospheric Science, University of Cambridge, Cambridge, UK.

D. Kley and S. Schmitgen, Institut für Chemie und Dynamik der Geosphære, Forschungszentrum Jülich, Jülich, Germany.